Muscle, Ligament, and Joint-Contact Forces at the Knee during Walking

KEVIN B. SHELBURNE[1], MICHAEL R. TORRY[1], and MARCUS G. PANDY[2,3]

[1]Steadman-Hawkins Research Foundation, Biomechanics Research Laboratory, Vail, CO; [2]Department of Biomedical Engineering, The University of Texas at Austin, Austin, TX; and [3]Department of Mechanical and Manufacturing Engineering, The University of Melbourne, Victoria, AUSTRALIA

ABSTRACT

SHELBURNE, K. B., M. R. TORRY, and M. G. PANDY. Muscle, Ligament, and Joint-Contact Forces at the Knee during Walking. *Med. Sci. Sports Exerc.*, Vol. 37, No. 11, pp. 1948–1956, 2005. **Purpose:** *In vivo* measurement of the forces and strains in human tissues is currently impracticable. Computer modeling and simulation allows estimates of these quantities to be obtained noninvasively. This paper reviews our recent work on muscle, ligament, and joint loading at the knee during gait. **Methods:** Muscle and ground-reaction forces obtained from a sophisticated computer simulation of walking were input into a detailed model of the lower limb to obtain ligament and joint-contact loading at the knee for one full cycle of gait. **Results:** Peak anterior cruciate ligament (ACL) force occurred in early stance and was mainly determined by the anterior pull of the patellar tendon on the tibia. The medial collateral ligament was the primary restraint to anterior tibial translation (ATT) in the ACL-deficient knee. ATT in the ACL-deficient knee can be reduced to the level calculated for the intact knee by increasing hamstrings muscle force. Reducing quadriceps force was insufficient to restore ATT to the level calculated for the intact knee. For both normal and ACL-deficient walking, the resultant force acting between the femur and tibia remained mainly on the medial side of the knee. The knee adductor moment was resisted by a combination of muscle and ligament forces. **Conclusion:** Knee-ligament loading during the stance phase of gait is explained by the pattern of anterior shear force applied to the leg. The distribution of force at the tibiofemoral joint is determined by the variation in the external adductor moment applied at the knee. The forces acting at the tibiofemoral and patellofemoral joints are similar during normal and ACL-deficient gait. Hamstrings facilitation is more effective than quadriceps avoidance in reducing ATT during ACL-deficient gait. **Key Words:** COMPUTER MODELING, TIBIOFEMORAL, PATELLOFEMORAL, MEDIAL COMPARTMENT, ADDUCTOR MOMENT, OSTEOARTHRITIS

Measurement of the forces and strains in human tissues is currently impracticable. *In vivo* measurements of joint motion, ground-reaction forces, and muscle EMG do not provide direct information about the forces developed by the muscles and the forces transmitted to the ligaments and bones. Although tissue forces can be monitored directly in cadaver specimens, the complex loading patterns applied to the knee during daily activity are difficult to reproduce in a cadaver model. Alternatively, mathematical modeling allows estimates of muscle, ligament, and joint loading to be obtained noninvasively. Detailed multisegment, multidegree-of-freedom models of the body have been used to determine muscle, ligament, and joint-contact loading in a range of activities, from rising from a squatting position (33) to normal walking (3).

A musculoskeletal model is an idealized mathematical representation of the body, comprising the bones, muscles, joints, and passive structures in varying degrees of complexity. A simulation is typically a computer program that uses the model to calculate the forces in the tissues and the corresponding movements of the joints (e.g., isokinetic knee extension exercise). Computer modeling and simulation can be viewed as an extension of the motion analysis experiment in two respects: first, as noted above, modeling and simulation can provide information that is not directly accessible by experimentation on humans; second, the model simulation data can be very helpful in explaining the results obtained from the motion analysis experiment. For example, modeling and simulation can be used to predict and explain the change in tibiofemoral compartment loads resulting from a measurable increase in the adductor moment at the knee (31). Data obtained from both *in vitro* and *in vivo* experiments are integral to the development and use of computer models. Musculoskeletal models are often developed based on measurements obtained from cadaver specimens; measurements of the geometry and mechanical properties of the muscles, ligaments, and bones are needed to replicate the behavior of the musculoskeletal system in a mathematical model of movement. *In vivo* motion analysis experiments, on the other hand, provide the means by which model response may be verified; for example, video data are often used to verify calculations of joint movement, whereas muscle EMG is important for validating calculations of the sequence and timing of muscle force (3).

Modeling and simulation techniques are being used increasingly either to explain an observed behavior of a phys-

Address for correspondence: Kevin Shelburne, PhD, Steadman-Hawkins Research Foundation, Vail, Colorado 81657; E-mail: kevin.shelburne@shsmf.org.
Submitted for publication January 2005.
Accepted for publication June 2005.

0195-9131/05/3711-1948/0
MEDICINE & SCIENCE IN SPORTS & EXERCISE®

DOI: 10.1249/01.mss.0000180404.86078.ff

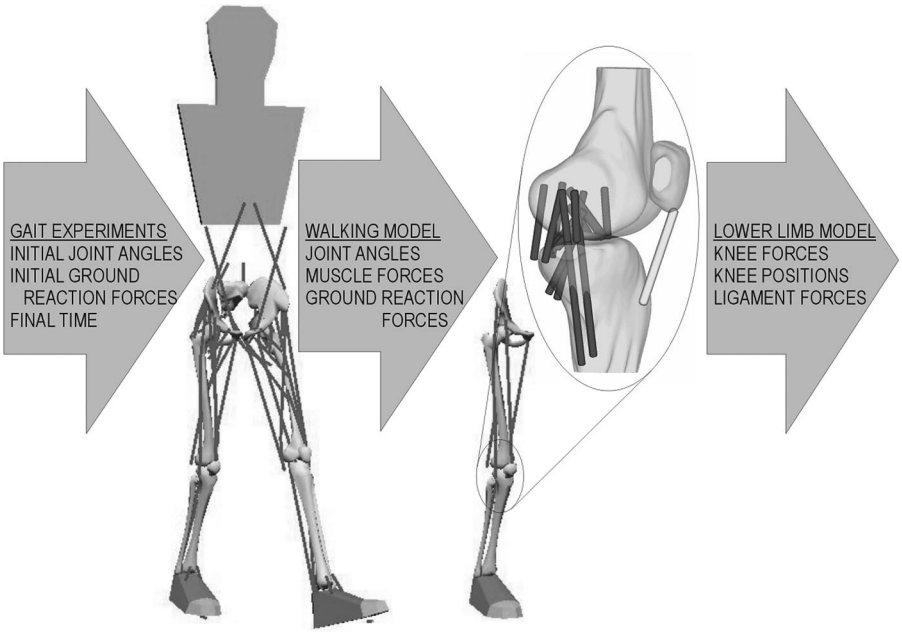

FIGURE 1—Initial conditions for the dynamic optimization solution for normal walking were obtained from gait measurements obtained from five male subjects, each of whom walked at his self-selected (normal) speed. Muscle forces, ground-reaction forces, and joint motion predicted by the dynamic optimization solution for normal walking were input to the lower-limb musculoskeletal model. Ligament forces and joint-contact loading at the knee were calculated using the three-dimensional model of the lower limb and knee.

ical system or to predict a behavior based on an expected change in the physical system. For example, model simulations have been used recently to explain how muscle forces affect ACL loading during walking (34) and when landing from a jump (29). Model simulations have also been used to predict how individual muscles may mechanically adapt in an ACL-deficient knee to provide joint stability during walking (36). The predictive power of modeling and simulation enables the testing of hypotheses in ways that cannot be achieved with either *in vivo* or *in vitro* experiments.

In this paper, we review our recent work related to muscle, ligament, and joint loading at the knee during gait (34–37). Our overall goal was to describe and explain muscle-ligament interactions in the normal and ACL-deficient knee when subjects walked at their preferred speeds. To accomplish this, muscle and ground-reaction forces obtained from a sophisticated simulation of walking were input into a detailed computer model of the lower limb to obtain ligament and joint-contact loading at the knee for one full cycle of gait. The specific aims of this paper are to summarize the results obtained for ligament and joint-contact loading in the intact knee during normal walking; to show how the secondary ligaments and capsular structures may be loaded in the ACL-deficient knee as muscle and ground-reaction forces are applied to the leg during gait; and to contrast the effects of quadriceps and hamstrings muscle actions on anterior tibial translation in the ACL-deficient knee during gait.

METHODS

Muscle, ligament, and joint-contact loads were calculated using a three-dimensional model of the lower limb (Fig. 1) (34). The model was described in detail by Shelburne et al. (34), so only a brief description is given here. Five rigid bodies were used to represent the right leg: thigh, patella, shank, hindfoot, and metatarsals. These segments were connected together by five joints: hip, tibiofemoral joint, patellofemoral joint, ankle, and metatarsal joint (Fig. 2). The hip, ankle, and metatarsal joints were modeled according to descriptions given by Anderson and Pandy (3), whereas the tibiofemoral and patellofemoral joints were each represented as a 6-*df* joint (28).

The geometry of the distal femur, proximal tibia, and patella was based on cadaver data reported for an average-size knee (12). The contacting surfaces of the femur and tibia were modeled as deformable, whereas those of the femur and patella were assumed rigid. The compressibility of the articular surfaces was adapted from measurements performed on cadavers (6). Fourteen elastic elements were used to describe the geometric and mechanical behavior of the knee ligaments and joint capsule. The ACL and PCL were each represented by an anterior and a posterior bundle. The MCL was represented by two layers: a superficial layer comprised of three bundles, and a deep layer comprised of two bundles. The lateral collateral ligament (LCL), popliteofibular ligament (PFL) and the anterolateral structures were each represented by one bundle, whereas the posterior capsule was represented by two: a medial and a lateral bundle. The elastic properties of each bundle were described by a nonlinear force-strain curve (6) and adjusted to match the measured laxity of the tibiofemoral joint obtained from cadaver experiments (28,34). A single elastic element modeling the contribution of the popliteofibular ligament (PFL) was added to the model described in Shelburne et al. (34). This element was placed in the knee model according to the anatomical descriptions given by Munshi et al. and Staubi et al. (26,39). The elastic properties of the model PFL were verified by simulating varus and external rotation movements of the knee as measured *in vitro* by Grood et al. (14).

Thirteen muscles were represented in the lower-limb model (Fig. 2A). The paths of all muscles except vasti,

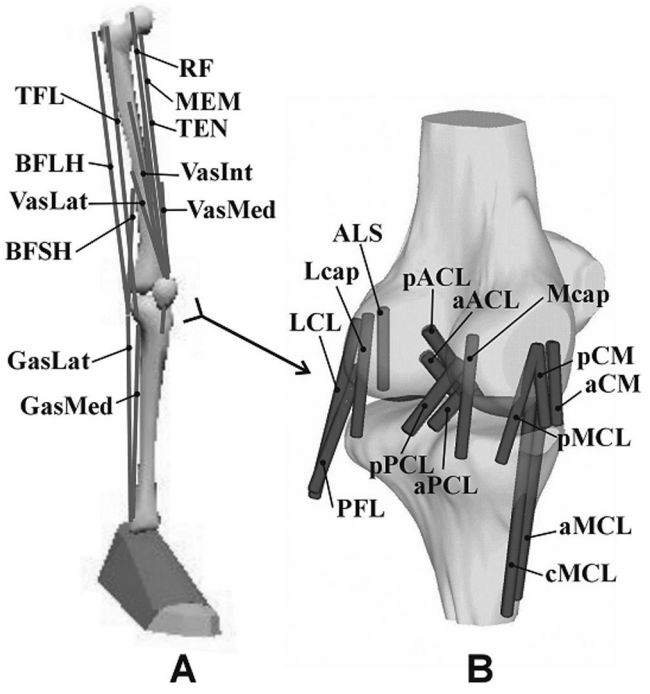

FIGURE 2—(A) The muscles of the leg were modeled by thirteen actuators (34): vastus medialis (VasMed), vastus intermedius (VasInt), vastus lateralis (VasLat), rectus femoris (RF), biceps femoris long head (BFLH), biceps femoris short head (BFSH), semimembranosus (MEM), semitendinosus (TEN), medial gastrocnemius (GasMed), lateral gastrocnemius (GasLat), and tensor fascia latae (TFL). Also included in the model but not shown are sartorius and gracilis. (B) The ligaments of the tibiofemoral joint were modeled by fourteen elastic bundles (34): anterior (aACL) and posterior (pACL) bundles of the anterior cruciate ligament; the anterior (aPCL) and posterior (pPCL) bundles of the posterior cruciate ligament; the anterior (aMCL), central (cMCL), and posterior (pMCL) bundles of the superficial medial collateral ligament; the anterior (aCM) and posterior (pCM) bundles of the deep medial collateral ligament; the lateral collateral ligament (LCL); the popliteofibular ligament (PFL); the anterolateral structures (ALS); and the medial (Mcap) and lateral (Lcap) posterior capsule.

hamstrings, and gastrocnemius were identical to those used by Anderson and Pandy (3). Whereas vasti, hamstrings, and gastrocnemius were each represented as one muscle in the walking model (3), the separate heads of each of these muscles were included in the current lower-limb model (34).

The joint motion, Ground-reaction forces, and muscle forces input to the lower limb model were obtained from a simulation of normal walking (3). The performance of the walking model was validated both statically and dynamically before it was used to simulate the gait cycle. First, the model was used to simulate maximum isometric contractions of the muscles crossing the ankle, knee, and hip; the parameters that determine musculoskeletal geometry (i.e., muscle moment arms) and muscle strength in the model were evaluated by comparing the maximum isometric torques calculated in the model against measurements of the same quantities obtained from subjects. The model was then used to simulate a weightbearing activity: vertical jumping. Maximum-height jumping was chosen because this particular task presents a relatively unambiguous performance criterion (jump height). ground-reaction forces and jump height computed in the model were quantitatively compared to values measured for five subjects who were instructed to "jump as high as possible" (2).

The dynamic optimization problem for normal walking was to find the muscle excitation histories, muscle forces, and body-segmental motions corresponding to minimum metabolic energy consumed per unit distance moved. Bilateral symmetry was assumed, and so only half the gait cycle was simulated. The model simulation began at left toe-off and proceeded through right toe-off. The initial states of the model were obtained from gait experiments performed on 5 male subjects (see below). The final time was fixed to 0.56 s, which was the average time taken by the subjects to complete one half the gait cycle. Terminal constraints were applied to the joint angles, joint angular velocities, and muscle forces to enforce symmetry of the gait cycle. Details of the dynamic optimization problem are given by Anderson and Pandy (3). Details of the model used to estimate muscle metabolic energy consumption are presented by Bhargava et al. (5). A computational solution was found by converting the dynamic optimization problem to a parameter optimization problem (27). The model simulation results were shown to be consistent with kinematic, force plate, and muscle EMG measurements recorded for five male subjects, each of whom walked at his self-selected (normal) speed (3).

The initial states of the model were found by averaging kinematic and force plate data obtained from the gait experiments. The average age, height, and mass of the subjects was 26 ± 3 yr, 177 ± 3 cm, and 70.1 ± 7.8 kg, respectively. Passive reflective markers were placed on both the left and right sides of the body to measure the three-dimensional positions of the segments. Pairs of preamplified EMG surface electrodes (Iomed Inc., Salt Lake City, UT) were attached to the right leg and torso to record activity in 11 muscles. Simultaneous video, forceplate, and EMG data were recorded for five walking trials of each subject. The positions of the markers were recorded using a four-camera video-based motion capture system (Motion Analysis Inc., Santa Rosa, CA). Joint angles were calculated from the three-dimensional marker coordinates. Ground reaction forces and moments were measured using a six-component, strain gauge force platform (Bertec Inc., Columbus, OH). Before data collection, the step frequency of each subject was measured as they walked around a 400-m outdoor track. Step frequency was reproduced in the laboratory by setting a metronome to the subject's measured outdoor step frequency. The joint angles, velocities, and accelerations, and ground-reaction force of the model at left toe-off was set to the average values recorded for the subjects. The corresponding initial values of the muscle activations and forces were computed by solving a static optimization problem at the instant of left toe-off.

Inverse dynamics was used to determine joint-contact loading and the relative positions of the bones at the knee at each instant during the gait cycle. Specifically, the joint angles, ground forces, and muscle forces obtained from the walking simulation (3) were applied to the lower-limb model, and a static equilibrium problem was then solved to find the anterior–posterior and medial–lateral translations,

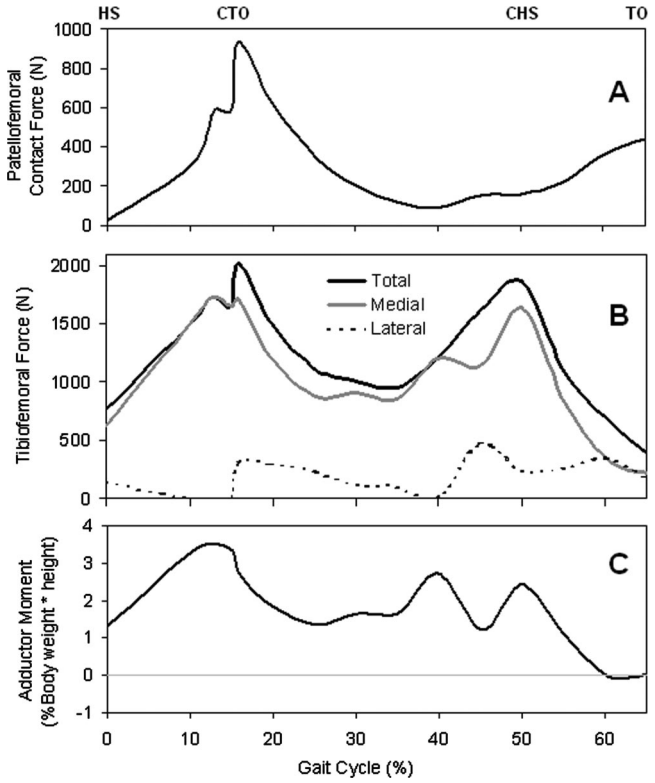

FIGURE 3—(A) Total force acting between the patella and femur during normal walking. Acronyms at the top of the figure mark the temporal progression of events during the gait cycle: heel-strike (HS), contralateral toe-off (CTO), contralateral heel-strike (CHS), and toe-off (TO). (B) Total tibiofemoral joint load calculated for the stance phase of normal walking. The *gray* and *dashed lines* show the forces acting in the medial and lateral compartments of the knee, respectively. (C) External adductor moment applied about the knee during the stance phase of normal walking. The external adductor moment was defined as the moment produced by the ground-reaction force about the center of the knee in the frontal plane.

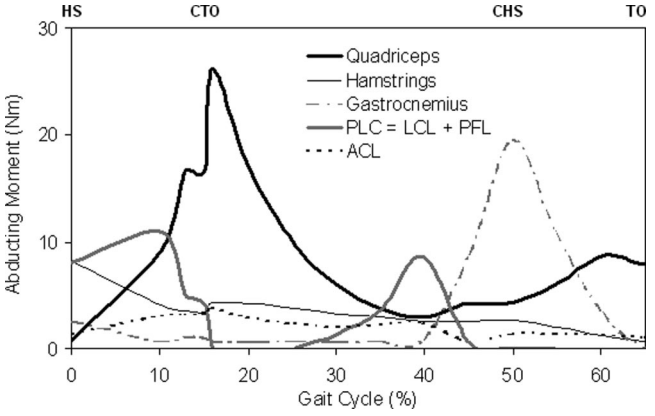

FIGURE 4—The *abductor* moment produced by the muscles and ligaments spanning the knee. The abductor moment is the moment needed to resist the external adductor moment acting about the knee.

varus–valgus orientation, joint-contact forces, and ligament forces at the knee. Details of the solution procedure can be found in Shelburne et al. (34).

RESULTS AND DISCUSSIONS

Intact knee. Peak patellofemoral force calculated for normal walking in the model was 12.51 $N \cdot kg^{-1}$, which coincided with the appearance of peak quadriceps force at contralateral toe-off (CTO) (Fig. 3A). These results are in general agreement with findings by Heino-Brechter and Powers (18), who reported peak values of patellofemoral force ranging from 9.51 $\pm$ 1.24 $N \cdot kg^{-1}$ for walking at normal speeds to 13.37 $\pm$ 1.16 $N \cdot kg^{-1}$ for fast walking. Heino-Brechter and Powers also found peak patellofemoral contact forces to occur near CTO.

In agreement with previous studies, the model calculations showed a bimodal pattern for tibiofemoral contact force (Fig. 3B), with the first and second peaks aligning with peak forces developed by the quadriceps and gastrocnemius muscles. The calculations also showed that the center of pressure at the knee was concentrated on the medial side, which is consistent with findings reported by others (16,19,25). Compressive force acting between the femur and tibia was much greater in the medial compartment than in the lateral compartment throughout the stance phase of gait. The compressive force was much greater on the medial side because the resultant ground-reaction force passed medial to the knee at all times during stance. The medially directed ground-reaction force created an external moment that acted to adduct the knee in the frontal plane (19,31) (Fig. 3C). The adduction moment has been reported as a key determinant of the distribution of tibiofemoral load between the medial and lateral sides of the knee (17,19,25,31).

The external knee adductor moment was resisted by a combination of muscle and ligament forces (Fig. 4). The quadriceps provided most of the resistance in the first half of stance, whereas the gastrocnemius contributed most of the resisting muscular moment thereafter (Fig. 4). Although their study did not include weightbearing, Lloyd and Buchanan (23) also found that the quadriceps muscles provided the majority of the muscular moment needed to resist an adduction moment applied during knee extension.

Ligaments provided significant resistance to the external knee adductor moment immediately after heel strike and during midstance (Fig. 4). Schipplein and Andriacchi (31) found that the adductor moment was resisted by the passive lateral supporting structures of the knee for nearly 60% of the stance phase of gait. The contribution of ligament to resist adduction moment during walking was highest when muscle force (and muscular flexion–extension moment) was lowest (e.g., compare PLC force with that in the muscles at 40% of the gait cycle in Fig. 4). Likewise, Lloyd and Buchanan (23) showed that when the knee flexion–extension moment of seated subjects was small, only about 15% of an applied adduction moment was resisted by the action of the muscles.

The posterior lateral corner (PLC) ligaments, which were represented by the lateral collateral ligament (LCL) and the popliteofibular ligament (PFL), provided the primary passive restraint to lateral joint opening in the model (Fig. 4). Peak forces borne by the LCL and PFL were 167 and 15 N, respectively, which are well below the failure strengths

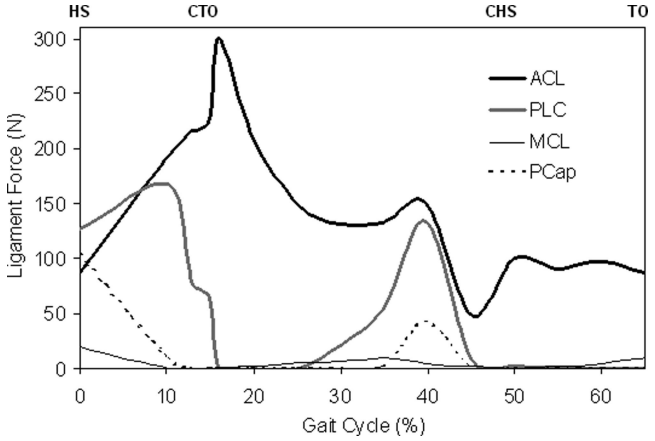

FIGURE 5—Forces transmitted to the cruciate ligaments, the collateral ligaments, and the posterior capsule of the knee during normal walking. The ACL bore the largest force: peak force transmitted to the ACL was around one half of body weight at contralateral toe-off.

reported for these structures (1). Although the peak force borne by the anterior cruciate ligament (ACL) in the model was much higher than that calculated for the PLC, the ability of the ACL to resist the external adductor moment at the knee was much less (compare ACL and PLC in Figs. 4 and 5).

The pattern of force calculated for the PLC was similar to that obtained for the external adductor moment at the knee (cf. Fig. 3C and Fig. 5). PLC force was highest at times when the external adductor moment was high and the resistance provided by the muscles was low (near foot-flat and before heel-off in Figs. 3C and 4). This is consistent with results obtained from cadaver experiments, which show that the PLC plays an important role in resisting adductor moments applied at the knee (14,24,44,46).

The anterior cruciate ligament (ACL) was loaded throughout the stance phase of gait (Fig. 5). Peak ACL force occurred at CTO and was estimated to be 303 N, which is about 13% of the reported failure strength of the ligament (38). The computed pattern of ACL loading was similar to that predicted by Collins (8), Collins and O'Connor (9), Harrington (16), and Morrison (25). However, there are significant differences in the predicted values of peak ACL force. Morrison calculated a maximum ACL force of 156 N (~0.2 BW), whereas Harrington predicted forces of about 411 N (~0.7 BW), and Collins and O'Connor and Collins obtained even higher forces in the range of 1.5–3.5 and 1.3–1.7 BW, respectively. Peak ACL force for normal walking obtained in the current study was less than one half of BW, and was similar to the levels of ACL loading predicted for isokinetic knee-extension exercise at fast speeds (34). The force induced in the ACL was explained by the balance of muscle forces, joint-contact forces, and the ground-reaction force applied to the leg; each of these forces contributed to the resultant shear force acting at the knee. The patellar tendon, gastrocnemius, and tibiofemoral contact force all applied anterior shear forces to the leg, whereas hamstrings and the resultant ground-reaction force applied posterior shear forces. The resultant shear force contributed by all sources other than the knee ligaments and inertial forces was directed anteriorly throughout stance (Fig. 6, shaded region).

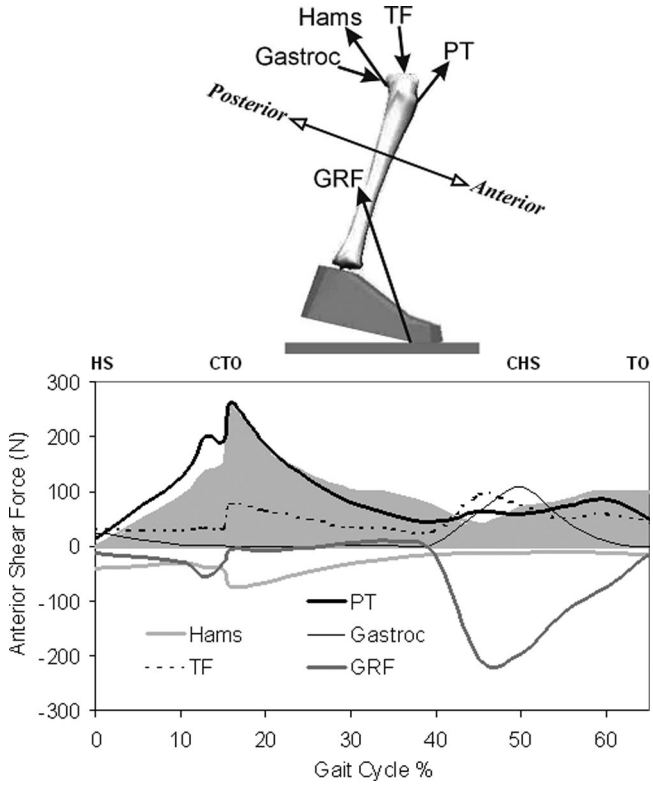

FIGURE 6—Shear forces acting on the lower leg. The *shaded region* shows the total shear force borne by the knee ligaments in the model. Total shear force is the shear force due to the muscle forces, ground-reaction forces, and joint-contact forces. Anterior shear forces tended to translate the leg anteriorly; posterior shear forces tended to translate the leg posteriorly. Hamstrings always applied a posterior shear force to the leg because these muscles pass behind the knee and insert on the back of the tibia. The ground-reaction force applied a posterior shear force to the leg because the line of action of the resultant ground force passed behind the knee as indicated in the diagram above the graph. Symbols appearing in the diagram are PT (patellar tendon), HAMS (hamstrings); Gastroc (gastrocnemius), TF (tibiofemoral contact force), and GRF (ground-reaction force).

The model ACL was loaded whenever the resultant shear force pointed anteriorly. In early stance, the shear force from the patellar tendon dominated the resultant shear force applied to the leg, and so maximum force was transmitted to the ACL at this time. Patellar tendon shear force was large in early stance because quadriceps force was large and also because the line of action of the patellar tendon was inclined anteriorly relative to the long axis of the tibia (32). ACL force was relatively small in late stance because the posterior component of the ground-reaction force was nearly equal to the sum of the anterior shear forces supplied by the patellar tendon, gastrocnemius, and the tibiofemoral contact force at that time (Fig. 6). Gastrocnemius applied an anterior shear force to the shank because the knee was nearly fully extended just before contralateral heel strike, and at small flexion angles gastrocnemius wraps around the back of tibia (11,32). Tibiofemoral contact force applied an anterior shear force to the leg due to the posterior slope of the tibial plateau (13,32). The ground-reaction force applied a posterior shear force to the leg because the line of action of the resultant ground force passed behind the knee. The posterior shear force caused by the ground reaction increased before con-

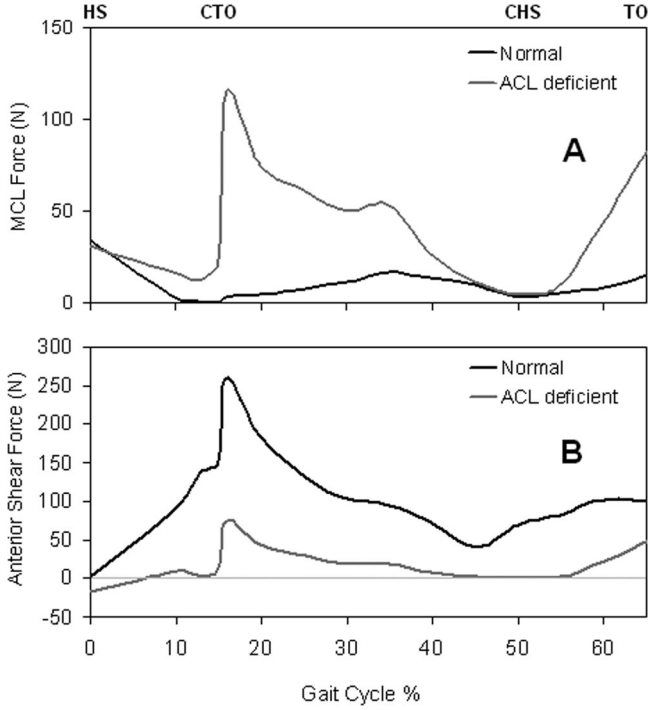

FIGURE 7—(A) Force transmitted to the medial collateral ligament in the normal and ACL-deficient knee during walking. (B) Net anterior shear force applied to the tibia during ACL-deficient gait compared with that calculated from the model for normal gait.

tralateral heel strike because the angle between the shank and the ground increased at this time.

The model posterior cruciate ligament (PCL) was unloaded during stance because the resultant shear force at the knee pointed anteriorly at this time (Fig. 6). This result of the model correlates with the clinical observation that the knee often responds adequately to conservative treatment after isolated rupture of the PCL, without the need for reconstruction (41,42,45).

Peak force borne by the medial collateral ligament (MCL) was less than 20 N during stance (Fig. 5). The model MCL was not loaded much for two reasons: first, the ACL provided the primary restraint to anterior tibial translation in the intact knee; and second, the ground-reaction force applied an adductor moment to the leg, which could only be resisted by the structures on the lateral side of the knee.

ACL-deficient knee. Removing the ACL from the model caused MCL force to increase significantly, so much so that it became the primary restraint to anterior tibial translation in the ACL-deficient (ACLd) knee (Fig. 7). This finding is consistent with results obtained from the *in vitro* experiments of Haimes et al. (15) and Sullivan et al. (40). These researchers recorded a significant increase in ATT in the ACLd knee when the MCL was removed, showing that the MCL provides primary restraint to ATT in the ACLd knee. Peak force borne by the MCL in the ACLd knee was nearly four times greater than that calculated for the intact knee. (Kanamori et al. (20) calculated a twofold increase in MCL force when a 134-N anterior shear force was applied to a cadaver knee subsequent to section of the ACL.) Nonetheless, peak force borne by the MCL in the ACLd knee was less than half that estimated for the ACL in the intact knee (compare MCL in Fig. 7A with ACL in Fig. 5). In contrast, peak force calculated for the PLC in the ACLd knee was roughly the same as that predicted for the intact knee. Even though the peak force transmitted to the MCL increased by a factor of four when the model ACL was removed, this value was still significantly less than the breaking strength reported for the MCL (7). This is because the magnitude of the resultant anterior shear force acting at the knee decreased when the ACL was removed. Anterior shear force decreased because the patellar tendon angle was smaller in the ACLD knee. The patellar tendon angle was smaller because anterior tibial translation increased when the model ACL was removed. As a result, the patellar tendon applied a smaller anterior shear force to the tibia, which caused the resultant anterior shear force to be lower (Fig. 7B).

Peak patellofemoral joint-reaction force was 14% lower at contralateral toe-off in the ACLd knee compared with that calculated for the intact knee. An increase in anterior tibial translation in the ACLd knee caused the quadriceps tendon and patellar tendon to become less steeply inclined to the long axis of the patella, which decreased the contact force acting between the patella and femur. Peak tibiofemoral joint-reaction force was 5% lower in the ACLd knee than in the intact knee, much less than that calculated for the patellofemoral joint. Tibiofemoral joint-reaction force was lower in the ACLd knee because the component of ACL tension acting to pull the tibia and femur together was nonexistent. In the frontal plane, the location of the center of pressure on the medial side of the knee did not change much when the model ACL was removed. In the sagittal plane, the location of tibiofemoral load on the medial and lateral sides of the tibial plateau shifted posterior because ATT increased as noted above. The role of the PLC was the same in the ACLd knee as in the intact knee: it contributed most of the resistance to the external adductor moment applied to the leg during stance. PLC force increased only a small amount in the ACLd knee.

Quadriceps avoidance versus hamstrings facilitation. Some studies have suggested that a reduction in the knee extensor moment, brought about by a decrease in quadriceps muscle activation, is an effective strategy for limiting anterior tibial translation during ACLd gait (4). To test this hypothesis, quadriceps force was decreased in the model and anterior tibial translation recalculated to determine whether a change in quadriceps force alone could reduce ATT in the ACLd knee to the amount calculated for the intact knee. The model simulation results showed that it was not entirely possible to restore ATT in the ACLd knee to the amount calculated for normal gait merely by reducing the magnitude of quadriceps force. There were periods near heel strike and in midstance when the lower limit of quadriceps force (zero force) was reached, and yet ATT in the ACLd knee was still greater than that obtained for the intact knee (36). The calculated decrease in quadriceps force resulted in complete elimination of the knee extensor moment (a quadriceps avoidance pattern) (Fig. 8A).

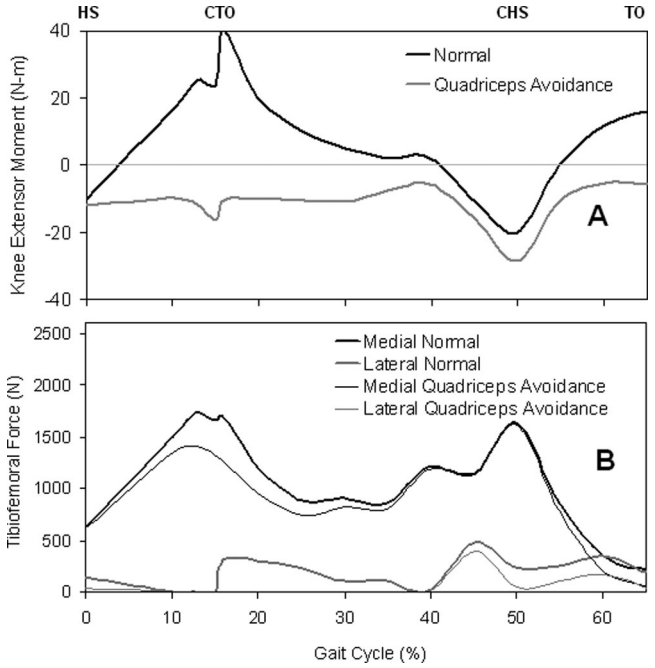

FIGURE 8—(A) Knee extensor moment calculated for normal walking compared to that calculated when quadriceps force was decreased (quadriceps avoidance) to achieve a normal level of anterior tibial translation (ATT) during ACLd gait. (B) Forces acting in the medial and lateral compartments of the knee during normal gait compared to those calculated for quadriceps avoidance during ACLd gait.

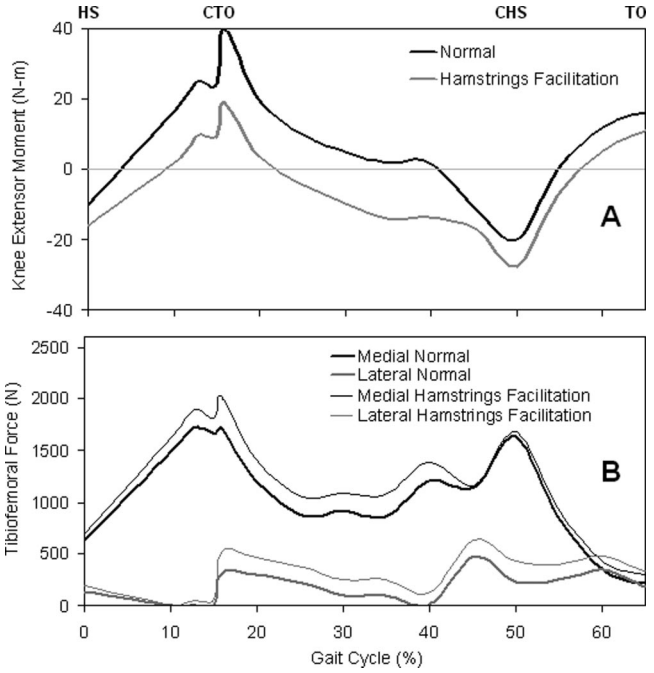

FIGURE 9—(A) Knee extensor moment calculated for normal walking compared with that calculated when hamstrings muscle force was increased (hamstrings facilitation) to achieve a normal level of ATT during ACLd gait. (B) Forces acting in the medial and lateral compartments of the knee during normal gait compared with those calculated for hamstrings facilitation during ACLd gait.

Reducing the force in the quadriceps meant that less force was transmitted between the femur and tibia in the model (Fig. 8B). Although the peak force in the medial compartment decreased by 313 N at contralateral toe off (Fig. 8B, compare thin and thick black lines at CTO), practically all of the contact force acting between the femur and tibia was transmitted on the medial side of the knee (compare thin black and gray lines in Fig. 8B). As a consequence, the ligaments were required to provide even greater resistance to the external adductor moment than that calculated for the intact knee; peak force borne by the PLC in the ACLd knee was two times greater than that predicted for the intact knee when the quadriceps muscles were deactivated.

Very few studies have quantified the effect of muscle compensation on knee instability during ACLd gait. Using a two-dimensional model of the lower limb, Liu and Maitland (22) found that 56% of peak isometric hamstrings force was necessary to restore ATT in the ACLd knee to the amount observed in normal gait. This analysis, however, was performed for a single instant of the gait cycle (heel strike) and considered only the effect of hamstrings muscle action on ATT when people walked at their self-selected speeds. To evaluate the effect of hamstrings muscle compensation on ATT during ACLd walking, hamstrings force was increased in the model and ATT recalculated to determine whether a change in hamstrings force alone could reduce ATT in the ACLd knee to the amount calculated for the intact knee. The calculations showed that it was possible to reduce ATT to the level calculated for the intact knee merely by increasing the magnitude of hamstrings force. As expected, an increase in hamstrings force led to a decrease in the knee extensor moment, but the drop in extensor moment was much less dramatic than that obtained for simulated quadriceps avoidance (compare gray lines in Fig. 8A and 9A).

An increase in hamstrings force caused an increase in the resultant force acting at the tibiofemoral joint during ACLd gait; the peak force transmitted on the medial side of the knee increased by 307 N (Fig. 9B). Although an increase in hamstrings force meant that the leg muscles provided more resistance to the adductor moment acting about the knee, this did not significantly alter the peak force borne by the PLC. PLC force remained about the same because hamstrings force was not increased substantially near foot-flat and before heel-off, when PLC resistance to adductor moment was highest.

Whereas our results support the contention that either isolated quadriceps or hamstrings muscle action can stabilize the ACLd knee during walking, they also suggest that the latter is more effective in reducing ATT during ACLd gait. Given that quadriceps avoidance is usually accompanied by quadriceps muscle weakness, which has been associated with medial compartment joint degeneration (21), a hamstrings facilitation pattern would appear to be more effective on these grounds as well. Importantly, both compensatory strategies change not only the resultant force at the tibiofemoral joint, but also the way this load is shared between the soft tissues and the medial and lateral sides of the knee.

Limitations. The limitations associated with estimating muscle forces during walking have been described by Anderson and Pandy (3), whereas those pertaining to the

knee model used to calculate ligament and joint-contact forces have been outlined by Pandy et al. (28) and Shelburne et al. (34). What is perhaps most relevant to the results presented here are the limitations associated with the model predictions of muscle and ligament loading in ACLd gait. The model simulation results did not take into account gait alterations that are known to occur following loss of the ACL, alterations that include, for example, increased knee flexion during stance (10). Thus, the joint angles, ground forces, muscle forces, and joint-reaction forces input to the ACLd model were assumed to be identical with those measured in normal gait. This assumption may be justifiable on two grounds: first, many ACLd patients exhibit near normal kinematics and kinetics during walking (30,43); and second, there is currently no clear consensus regarding the existence of a general adaptive strategy in patients who walk without an ACL. Normal kinematic profiles were also assumed in the model calculations of muscular compensation during ACLd gait. We chose to exclude alterations in joint kinematics from these analyses, because we wanted to examine the effects of adaptations in quadriceps and hamstrings muscle action alone. Our overall goal was to test the hypothesis that a change in either quadriceps or hamstrings muscle force is sufficient to stabilize the ACLd knee during walking. By increasing or decreasing thigh muscle force in the static equilibrium calculations, and keeping all other conditions the same, we were able to isolate this effect. More research is needed to evaluate the effects of simultaneous changes in joint kinematics and thigh muscle force on ATT during ACLd gait.

CONCLUSIONS

The forces transmitted to the knee ligaments during the stance phase of normal walking are explained mainly by the patterns of anterior shear force and varus moment applied to the leg. The pattern of force in the ACL is explained almost entirely by the anterior pull of the patellar tendon, whereas that in the posterior lateral corner results mainly from a medially directed ground-reaction force, which applies an adductor moment to the leg. When the ACL is absent, the maximum force transmitted to the MCL increases by a factor of four, but it nevertheless remains well below the failure strength of the ligament. The magnitude of force transmitted to the MCL remains limited in the ACLd knee, because the magnitude of the resultant anterior shear force decreases significantly relative to that present in the intact joint. These results suggest that whereas the MCL acts as the primary restraint to anterior tibial translation in the ACLd knee, it may still function safely in activities like walking. The model calculations also indicate that the forces acting at the tibiofemoral and patellofemoral joints are not very different in normal and ACLd walking. The reason is that the ACL does not act to resist much of the varus moment applied by the external ground-reaction force. However, the location of tibiofemoral force on the medial and lateral sides of the tibial plateau is moved posterior by the increase in anterior tibial translation in the ACLd knee. Hamstrings facilitation is more effective than quadriceps avoidance in reducing anterior tibial translation during ACLd gait. Both forms of muscle compensation potentially alter the distribution of load across the tibiofemoral joint. Quadriceps avoidance can increase the force transmitted to the PLC by a factor of two because these muscles then offer less resistance to the external adductor moment acting about the knee.

This work was supported in part by the Steadman-Hawkins Sports Medicine Foundation, the Department of Biomedical Engineering at The University of Texas at Austin, the Department of Mechanical Engineering at The University of Melbourne (Australia), the National Science Foundation Engineering Research Centers Grant EEC-9876363, and Sulzer Orthopedics Inc., Austin, Texas.

Based on the keynote delivered to the ACSM 2004 annual meeting: "Exploring Knee Mechanics with Modeling and Simulation."

REFERENCES

1. Amis, A. A., A. M. Bull, C. M. Gupte, I. Hijazi, A. Race, and J. R. Robinson. Biomechanics of the PCL and related structures: posterolateral, posteromedial and meniscofemoral ligaments. *Knee. Surg. Sports Traumatol. Arthrosc.* 11:271–281, 2003.
2. Anderson, F. C., and M. G. Pandy. A Dynamic Optimization Solution for Vertical Jumping in Three Dimensions. *Comput. Methods Biomech. Biomed. Engin.* 2:201–231, 1999.
3. Anderson, F. C., and M. G. Pandy. Dynamic optimization of human walking. *J. Biomech. Eng.* 123:381–390, 2001.
4. Berchuck, M., T. P. Andriacchi, B. R. Bach, and B. Reider. Gait adaptations by patients who have a deficient anterior cruciate ligament. *J. Bone Joint Surg. Am.* 72:871–877, 1990.
5. Bhargava, L. J., M. G. Pandy, and F. C. Anderson. A phenomenological model for estimating metabolic energy consumption in muscle contraction. *J. Biomech.* 37:81–88, 2004.
6. Blankevoort, L., J. H. Kuiper, R. Huiskes, and H. J. Grootenboer. Articular contact in a three-dimensional model of the knee. *J. Biomech.* 24:1019–1031, 1991.
7. Butler, D. L., F. R. Noyes, and E. S. Grood. Ligamentous restraints to anterior-posterior drawer in the human knee. A biomechanical study. *J. Bone Joint Surg. Am.* 62:259–270, 1980.
8. Collins, J. J. The redundant nature of locomotor optimization laws. *J. Biomech.* 28:251–267, 1995.
9. Collins, J. J., and J. J. O'Connor. Muscle-ligament interactions at the knee during walking. *Proc. Inst. Mech. Eng. [H].* 205:11–18, 1991.
10. Devita, P., T. Hortobagyi, J. Barrier, et al. Gait adaptations before and after anterior cruciate ligament reconstruction surgery. *Med. Sci. Sports Exerc.* 29:853–859, 1997.
11. Fleming, B. C., P. A. Renstrom, G. Ohlen, et al. The gastrocnemius muscle is an antagonist of the anterior cruciate ligament. *J. Orthop. Res.* 19:1178–1184, 2001.
12. Garg, A., and P. S. Walker. Prediction of total knee motion using a three-dimensional computer-graphics model. *J. Biomech.* 23:45–58, 1990.
13. Giffin, J. R., T. M. Vogrin, T. Zantop, S. L. Woo, and C. D. Harner. Effects of increasing tibial slope on the biomechanics of the knee. *Am. J. Sports Med.* 32:376–382, 2004.
14. Grood, E. S., S. F. Stowers, and F. R. Noyes. Limits of movement in the human knee. Effect of sectioning the posterior cruciate ligament and posterolateral structures. *J.Bone Joint Surg. Am.* 70:88–97, 1988.
15. Haimes, J. L., R. R. Wroble, E. S. Grood, and F. R. Noyes. Role of the medial structures in the intact and anterior cruciate ligament-deficient knee. Limits of motion in the human knee. *Am. J. Sports Med.* 22:402–409, 1994.

16. HARRINGTON, I. J. A bioengineering analysis of force actions at the knee in normal and pathological gait. *Biomed. Eng.* 11:167–172, 1976.
17. HARRINGTON, I. J. Static and dynamic loading patterns in knee joints with deformities. *J. Bone Joint Surg. Am.* 65:247–259, 1983.
18. HEINO BRECHTER, J., and C. M. POWERS. Patellofemoral stress during walking in persons with and without patellofemoral pain. *Med. Sci. Sports Exerc.* 34:1582–1593, 2002.
19. HURWITZ, D. E., D. R. SUMNER, T. P. ANDRIACCHI, and D. A. SUGAR. Dynamic knee loads during gait predict proximal tibial bone distribution. *J. Biomech.* 31:423–430, 1998.
20. KANAMORI, A., M. SAKANE, J. ZEMINSKI, T. W. RUDY, and S. L. WOO. In-situ force in the medial and lateral structures of intact and ACL- deficient knees. *J. Orthop. Sci.* 5:567–571, 2000.
21. LEWEK, M. D., K. S. RUDOLPH, and L. SNYDER-MACKLER. Quadriceps femoris muscle weakness and activation failure in patients with symptomatic knee osteoarthritis. *J. Orthop. Res.* 22:110–115, 2004.
22. LIU, W., and M. E. MAITLAND. The effect of hamstring muscle compensation for anterior laxity in the ACL-deficient knee during gait. *J. Biomech.* 33:871–879, 2000.
23. LLOYD, D. G., and T. S. BUCHANAN. A model of load sharing between muscles and soft tissues at the human knee during static tasks. *J. Biomech. Eng.* 118:367–376, 1996.
24. MARKOLF, K. L., J. S. MENSCH, and H. C. AMSTUTZ. Stiffness and laxity of the knee–the contributions of the supporting structures. A quantitative in vitro study. *J. Bone Joint Surg. Am.* 58:583–594, 1976.
25. MORRISON, J. B. The mechanics of the knee joint in relation to normal walking. *J. Biomech.* 3:51–61, 1970.
26. MUNSHI, M., M. L. PRETTERKLIEBER, S. KWAK, G. E. ANTONIO, D. J. TRUDELL, and D. RESNICK. MR imaging, MR arthrography, and specimen correlation of the posterolateral corner of the knee: an anatomic study. *AJR Am. J. Roentgenol.* 180:1095–1101, 2003.
27. PANDY, M. G., F. C. ANDERSON, and D. G. HULL. A parameter optimization approach for the optimal control of large- scale musculoskeletal systems. *J. Biomech. Eng.* 114:450–460, 1992.
28. PANDY, M. G., K. SASAKI, and S. KIM. A Three-Dimensional Musculoskeletal Model of the Human Knee Joint. Part 1: Theoretical Construct. *Comput. Methods Biomech. Biomed. Engin.* 1:87–108, 1998.
29. PFLUM, M. A., K. B. SHELBURNE, M. R. TORRY, M. J. DECKER, and M. G. PANDY. Model prediction of anterior cruciate ligament force during drop-landings. *Med. Sci. Sports Exerc.* 36:1949–1958, 2004.
30. ROBERTS, C. S., G. S. RASH, J. T. HONAKER, M. P. WACHOWIAK, and J. C. SHAW. A deficient anterior cruciate ligament does not lead to quadriceps avoidance gait. *Gait Posture* 10:189–199, 1999.
31. SCHIPPLEIN, O. D., and T. P. ANDRIACCHI. Interaction between active and passive knee stabilizers during level walking. *J. Orthop. Res.* 9:113–119, 1991.
32. SHELBURNE, K. B., and M. G. PANDY. A musculoskeletal model of the knee for evaluating ligament forces during isometric contractions. *J. Biomech.* 30:163–176, 1997.
33. SHELBURNE, K. B., and M. G. PANDY. A dynamic model of the knee and lower limb for simulating rising movements. *Comput. Methods Biomech. Biomed. Engin.* 5:149–159, 2002.
34. SHELBURNE, K. B., M. G. PANDY, F. C. ANDERSON, and M. R. TORRY. Pattern of anterior cruciate ligament force in normal walking. *J. Biomech.* 37:797–805, 2004.
35. SHELBURNE, K. B., M. G. PANDY, and M. R. TORRY. Comparison of shear forces and ligament loading in the healthy and ACL-deficient knee during gait. *J. Biomech.* 37:313–319, 2004.
36. SHELBURNE, K. B., M. R. TORRY and M. G. PANDY. The effect of muscle compensation on knee instability during ACL deficient gait. *Med Sci Sports Exerc.* 37:642–648, 2005.
37. SHELBURNE, K. B., M. R. TORRY, and M. G. PANDY. Contributions of muscle, ligament, and ground-reaction forces to tibiofemoral load during gait. *J. Orthop. Res.*, in press.
38. STAPLETON, T. R., J. I. WALDROP, C. R. RUDER, T. A. PARRISH, and T. E. KUIVILA. Graft fixation strength with arthroscopic anterior cruciate ligament reconstruction. Two-incision rear entry technique compared with one-incision technique. *Am. J. Sports Med.* 26:442–445, 1998.
39. STAUBLI, H. U., and S. BIRRER. The popliteus tendon and its fascicles at the popliteal hiatus: gross anatomy and functional arthroscopic evaluation with and without anterior cruciate ligament deficiency. *Arthroscopy* 6:209–220, 1990.
40. SULLIVAN, D., I. M. LEVY, S. SHESKIER, P. A. TORZILLI, and R. F. WARREN. Medial restrains to anterior-posterior motion of the knee. *J. Bone Joint Surg. Am.* 66:930–936, 1984.
41. TIBONE, J. E., T. J. ANTICH, J. PERRY, and D. MOYNES. Functional analysis of untreated and reconstructed posterior cruciate ligament injuries. *Am. J. Sports Med.* 16:217–223, 1988.
42. TORG, J. S., T. M. BARTON, H. PAVLOV and R. STINE. Natural history of the posterior cruciate ligament-deficient knee. *Clin Orthop* 246:208–216 1989.
43. TORRY, M. R., M. J. DECKER, H. B. ELLIS, K. B. SHELBURNE, W. I. STERETT, and J. R. STEADMAN. Mechanisms of compensating for anterior cruciate ligament deficiency during gait. *Med. Sci. Sports Exerc.* 36:1403–1412, 2004.
44. VELTRI, D. M., X. H. DENG, P. A. TORZILLI, R. F. WARREN, and M. J. MAYNARD. The role of the cruciate and posterolateral ligaments in stability of the knee. A biomechanical study. *Am. J. Sports Med.* 23:436–443, 1995.
45. WHIPPLE, T. L., and F. D. ELLIS. Posterior cruciate ligament injuries. *Clin. Sports Med.* 10:515–527, 1991.
46. WROBLE, R. R., E. S. GROOD, J. S. CUMMINGS, J. M. HENDERSON and F. R. NOYES. The role of the lateral extraarticular restraints in the anterior cruciate ligament-deficient knee. *Am. J. Sports Med.* 21: 257–262; discussion 263, 1993.